High overtone Bulk Acoustic Resonators: application to resonators, filters and sensors

Sylvain Ballandras, Thomas Baron, Eric Lebrasseur, Gilles Martin, Dorian Gachon, Alexandre Reinhardt, Pierre-Patrick Lassagne, Jean-Michel Friedt, Luc Chommeloux, David Rabus

ACOUSTICS 2012

High overtone Bulk Acoustic Resonators: application to resonators, filters and sensors

S. Ballandras[a], T. Baron[a], E. Lebrasseur[a], G. Martin[b], D. Gachon[c], A. Reinhardt[d], P.-P. Lassagne[d], J.-M. Friedt[a], L. Chommeloux[e] and D. Rabus[b]

[a]femto-st, 26 chemin de l'epitaphe, Equipe CoSyMa, 25000 Besançon, France
[b]Femto-st, 26 chemin de l'Epitaphe, 25030 Besançon, France
[c]Laboratoire PROMES-CNRS, UPR 8521, Rambla de la thermodynamique, 66100 Perpignan, France
[d]CEA LETI, CEA / Léti 17 rue des Martyrs 38054 Grenoble cedex 9
[e]SENSeOR SAS, Parc de Haute Technologie - Lot n°3 694, Avenue du Docteur Maur, 06250 Mougins, France
ballandr@femto-st.fr

Acoustelectric devices have been used now for several decades to stabilize oscillators, to filter radio-frequency signals or to allow for physical and even chemical detection and measurements. Among all the structures that have been developed in that purpose, one has been revealing particularly interesting for the development of high quality factor resonator on an extended range of frequency. It is based on the generation of high overtones in bulk acoustic wave resonant structure and therefore are currently called HBARs. These devices may be fabricated along various approaches but they always consist of a thin (or thinned) piezoelectric layer deposited or bonded onto a high quality single crystal material. The spectral response of this kind of device exhibit a periodic comb of peaks modulated by the transducer response, yielding resonances on a very large spectrum with various characteristics and properties. We present here the basic principles of such devices, their remarkable properties, the technologies required to manufacture them and the various applications they can be applied for. A focus is particularly dedicated to oscillator stabilization and to the development of wireless sensors.

Introduction

High overtone Bulk Acoustic Resonators (HBARs) are a sort of passive devices exploiting elastic waves propagating in a stratified substrate [1]. Such a substrate is composed of a piezoelectric thin (or thinned, as shown further) layer equipped with top and bottom electrodes bonded or deposited atop a thicker substrate. They have been developed along different approaches to take advantage of their extremely high quality factor. Until now, many investigations have been carried out using piezoelectric thin films (Aluminum Nitride – AlN, Zinc Oxide – ZnO) atop thick wafers of silicon or sapphire [2]. Although marginal, their application has been mainly focused on filters and frequency stabilization (oscillator) purposes, but the demonstration of their effective implementation for sensor applications has been achieved recently [4]. These devices maximize the Q factor that can be obtained at room temperature using elastic waves, yielding Quality factor times Frequency products close or slightly above 10^{14}, i.e. effective Q factors of about 100 000 at 1 GHz.

In this work, a presentation of the basic operation of HBARs is proposed to allow for introducing their remarkable properties and specificity. Therefore, a first section describes the overall operation principle of these devices. It is particularly shown how to develop single port as well as double port devices, allowing to replace SAW devices for most passive RF device applications. The following section is devoted to the implementation of such resonators and the related technologies are introduced. Although the preferred approach for fabricating such devices consists in depositing thin polycrystalline piezoelectric layers atop high acoustic quality single-crystal substrates [3], an approach based on single-crystal wafer bounding has revealed well suited for such development and therefore is presented in details in [3].

Once this technological approaches presented, the article focuses on effective implementation of HBARs for frequency filters which can be advantageously used as a stabilization element of oscillator loops. Various developments are illustrated in this section, showing the actual characteristics of single-crystal HBARs and their capability to provide high stability low phase noise oscillators. Another application finally is described concerning wireless sensor systems. The interest of this approach is illustrated and effective implementation are reported for temperature and force measurements.

As a conclusion, further development are discussed and the perspective to reach ultimate elastic properties of single crystal is considered.

HBAR principles

HBAR springs from the conjugation of the strong coupling coefficient of deposited piezoelectric thin films and of the high intrinsic quality of used substrates. The piezoelectric film and the two electrodes on its both sides are used as a transducer whereas the acoustic energy is mainly trapped in the substrate. The fundamental resonant frequency corresponds to a half wavelength mode in the entire thickness (fig.1) of the device and, in opposition to FBAR and SMR for which only odd harmonics exist, one can exploit both its odd and even harmonics which both satisfy the boundary conditions in that case. The main aspect of the resonator is due to the fact that the modes are much favorably excited near the resonance of the piezoelectric film itself and its odd harmonics than anywhere else in the spectrum. This yields electrical responses interpreted as the modulation of the piezoelectric film bulk mode resonance(s) modulated by the bulk modes of the whole stack, as shown in fig.2.

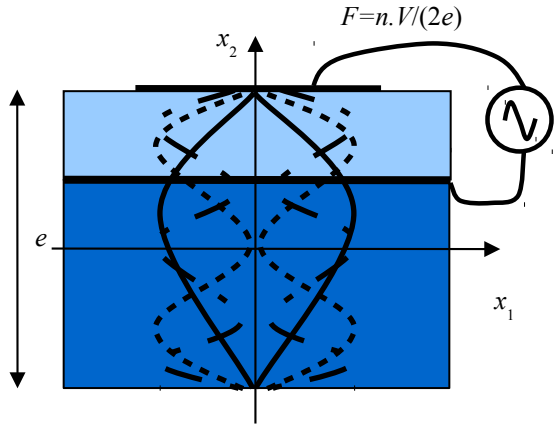

Figure 1: Scheme of a HBAR operation illustrating the energy distribution along the material stack, the fundamental mode develops in the whole structures and its odd and even harmonics can be excited

As explained in introduction, not only the above single port resonator structure can be achieved using HBARs but also double port structures can be implemented. The principle of such devices is inspired from the so-called monolithic filters based on coupled bulk waves in single crystals and illustrated in Fig.3. This is achieved by setting two resonators very close one another. The gap between these resonators must be narrow enough to allow for evanescent waves apart the resonator electrodes to recover and hence yielding mode coupling conditions. As both resonators operate similarly, they do present the same

spectral distribution and each harmonic bulk mode of the structure is identically coupled at almost exactly the same frequency.

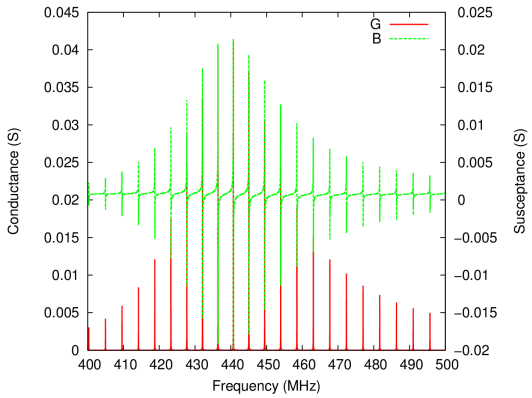

Figure 2: Theoretical admittance of a $LiNbO_3$/Quartz HBAR on a spectrum centered near the 434 MHz ISM band, showing numerous contributions located near the fundamental of the Lithium Niobate plate – note that only the odd harmonics of the transducer are excited, yielding the particular shape of the plotted admittance

The above mentioned coupling condition then favors for each coupled mode the existence of two distinct resonances corresponding to symmetrical and anti-symmetrical coupled modes in the structure composed by the two resonators. The width of the separation area then controls the spectral distance between the two coupled modes. This operation principle only holds if the resonator effectively traps the wave under its electrode, and therefore this condition must be validated by the analysis of dispersion modes, as shown in many text books and papers (see for instance [11]). Although this analysis was not conducted for this paper, the evanescent conditions are attested by the extremely high Q factor obtained using the tested configuration ((YX*l*)/36° $LiNbO_3$ thinned plate on (YX*l*)/36° $LiNbO_3$ substrate [4], [6]), i.e. more than 50 000 at 1.5 GHz.

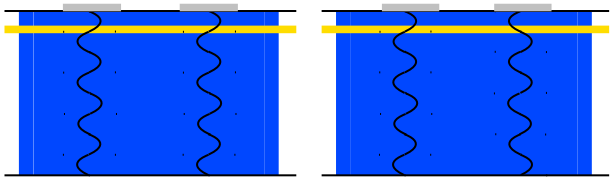

Figure 3: Principle scheme of the laterally-coupled-mode HBAR filter (a) symmetrical mode (b) anti-symmetrical mode

All these principles can be advantageously applied when controlling the technology for actual device development. This will be shown in the next section. Before that, some particular features that can be achieved by combining various single-crystal substrates are still discussed here. First, the possibility to control the Temperature Coefficient of Frequency (TCF) is presented. The celebrated Campbell&Jones method [9] is used here for predicting the TCFs of any mode of a given HBAR. As it has been reported hundred times in previous papers, only the main basic equation is reported below:

$$f = \frac{V}{2e} \rightarrow \frac{df}{f}(T) = \frac{dV}{V}(T) - \frac{de}{e}(T) \quad (1)$$

which means that the frequency changes due to temperature variations are computed as the difference between the development of the velocity and of the stack thickness vs temperature. As discussed in [7], Lithium Niobate and Quartz have been associated for the fabrication of shear-waver based HBARs. $LiNbO_3$ provides crystal orientations for which very strongly coupled shear waves exist (k_t^2 in excess of 45%) whereas AT cut of Quartz allows for compensating second order frequency-temperature effects. Although this idea was already proposed using other material combinations [5], no real design rules were reported until now and therefore the possibility to determine structures allowing for high frequency operation with first ordrer TCF (TCF_1) smaller than 1 ppm.K^{-1} was quite hypothetic. Second order compensation was even not imagined in [5]. Figure 4 shows the evolution of the TCF_1 of the first modes of thinned (YX*l*)/163° $LiNbO_3$ layer atop a (YX*lt*)/36°/90° Quartz plate for various Niobate/Quartz thickness ratios, always assuming a Lithium Niobate layer much thinner than the Quartz substrate (which allows for neglecting the differential thermoelastic stress within the stack). One can see that depending on the harmonic number, the TCF_1 changes from +1 to -14 ppm.K^{-1}. Furthermore, the TCF_1 is notably affected by the amount of energy coupled in the Lithium Niobate transducer and thus requires some attention when deriving design rules. Therefore, it is mandatory to accurately consider all the actual features of the structure for an accurate design of a resonator, i.e. the operation frequency, the harmonic number and the thickness ratio for a given structure. To complete this, one should also account for the effective thickness of the device as this parameter will control the possibility to select one (frequency/harmonic number) couple. Finally, it clearly appears that the analysis of such HBAR TCF requires a numerical analysis and that if an intuitive approach allows for a first order definition of crystal orientations, the complicated distribution of energy within the stack vs all the structure parameters induces more intrication in the design process.

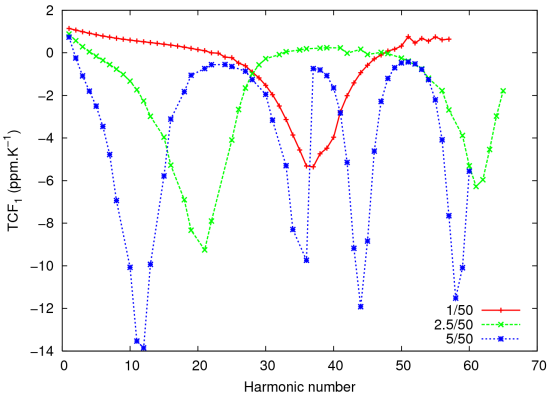

Figure 4: Plot of the TCF_1 of a HBAR built on a (YX*l*)/163° $LiNbO_3$ thinned plate bonded on (YX*lt*)/36°/90° Quartz substrate for various Niobate/Quartz thickness ratio (Quartz thickness arbitrary fixed to 50µm)

As an illustration of these considerations, the evolution of the TCF_1 of the most strongly coupled mode of the structure (coinciding with the fundamental mode of the

niobate plate alone) has been plotted vs niobate thickness (Fig.5). A TCF_1 vs Niobate/Quartz ratio law has been derived from this curve, yielding the following expression:

$$TCF_1 = 42.5 \times R_t + 3.2 \times \log(200\, R_t) \quad (2)$$

where R_t is the Niobate/Quartz ratio, thicknesses and TCF_1 being expressed in µm and in ppm.K^{-1} implicitly.

Considering now the TCF_1 evolution vs quartz cut angle θ (rotation around X axis), one can set the following complementary law:

$$TCF_1 = (\theta - 35.) \times 5.10^{-6} \quad (3)$$

Using these relations allows one to show that the most coupled mode of the structure is temperature compensated for R_t=1/50 for the (YX*lt*)/34°/90° quartz cut, whereas the (YX*lt*)/33°/90° and (YX*lt*)/32°/90° cuts will be selected for Rt respectively equal to 2.5/50 and 5/50.

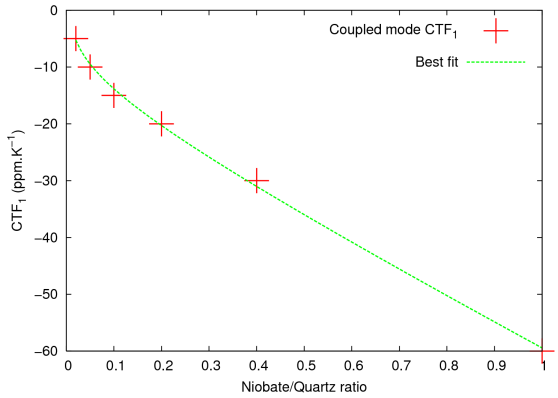

Figure 5: Plot of the TCF_1 of a HBAR built on a (YX*l*)/163° $LiNbO_3$ thinned plate bonded on (YX*lt*)/36/90 Quartz substrate for various Lithium Niobate/Quartz thickness ratio (Quartz thickness arbitrary fixed to 50µm)

Finally, a brief description is reported concerning pressure/stress measurements using HBARs. To better exemplify the adopted approach for such applications, one first considers as a reference usual Surface Acoustic Wave (SAW) stress and pressure sensors based on the frequency dependence of Rayleigh waves versus tensile stress at the surface of a membrane bent for instance by pressure. In the case of high overtone bulk waves propagating in such a structure, the stress/strain variations across the membrane thickness compensate the overall frequency variations in the whole stack. This can be easily demonstrated using for instance static finite element analysis with a very simple mesh as illustrated in fig.3. The strain and hence the stress actually change their signs along the membrane thickness, as shown in fig. 7. As a consequence, the strain variation across the HBAR generates velocity variations, on the one hand, the stress below the membrane neutral line yields an increase of resonant frequency of the HBAR, on the other hand, the stress above the neutral line yields a decrease of this frequency. Consequently, the resulting frequency shift is rather small and only based on the asymmetrical nature of the material stack.

In the case of a cantilever beam, one can imagine to manufacture a micro-cavity near the neutral line, without changing fundamentally its location. If the transducer of the HBAR structure is straight above this micro-cavity, the emitted bulk waves are reflected by this micro-cavity and hence confined in this membrane location. The micro-cavity then plays the role of a mirror for the waves, as illustrated in fig.8. First a standard HBAR structure is build and the defect located straight under the transducer location. This structure then is bonded on a plane wafer, yielding the expected material stack. The surface of the cavity should at minimum coincide strictly to the surface of the transducer, but to ease the fabrication (particularly to manage alignment issues) the cavity largely covers the transducer aperture.

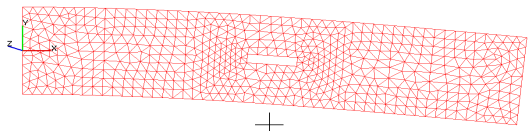

Figure 6: Cantilever beam submitted to bending force simulated by static finite element analysis. The defect in the middle of the beam is used further in the proposed development

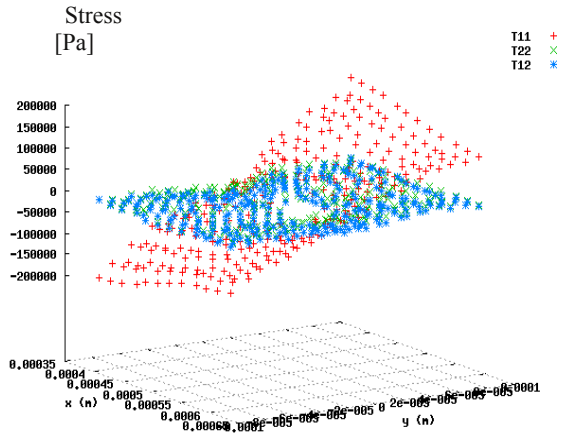

Figure 7: Stress variations as a function of the crystallographic direction.

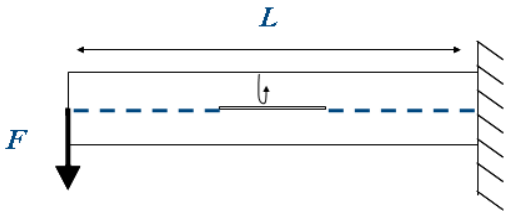

Figure 8: Waves and neutral line behaviors in the case of cantilever with micro-cavity and HBAR built above it.

As a conclusion of this theoretical section, one can prove that HBAR actually can be exploited in a similar way to SAW and further any kind of RF device based on piezoelectric coupling. The principal advantage of HBAR lies on the very small surface they need to be implemented for a given operation frequency. As a comparison, a 434 MHz SAW resonators on Quartz occupies a surface of about 6 to 10 mm2 whereas only a tenth of this surface is required for a HBAR operating at the same frequency. The main problem then consists in verifying the free surface condition on both side of the resonator. Various approaches are considered to address that problem based for instance

on flip-chip techniques yielding possible chip-size package developments.

Technology developments

Our process is based on the bonding of two single-crystal wafers. In this approach, we use optical quality polished surfaces to favor the bonding of the wafers. We start by a Chromium and Gold thin layer deposition by sputtering on both $LiNbO_3$ and Silicon wafers. The piezoelectric material wafer is then bonded onto the Silicon substrate via mechanical compression of the 200nm thick gold layers into an EVG wafer bonding machine as shown in fig. 9a. The bonding can be particularly controlled by adjusting the process duration and various parameters such as the applied pressure, the process temperature, the quality of the vacuum during the process, etc. We actually restrict the process temperature near a value close to the final thermal conditions seen by the device in operation. Since the exploited materials exhibit different thermal expansion coefficients, one must account for differential stresses when bonding both wafers and minimize them as much as possible. The piezoelectric wafer is subsequently thinned by lapping step to an overall thickness of 100 microns. The lapping machine used in that purpose and shown in fig. 9b is a SOMOS double side lapping/polishing machine based on a planetary motion of the wafers (up to 4" diameter) to promote abrasion homogeneity. We use an abrasive solution of silicon carbide. We can control the speed of the lapping by choosing the speed of rotation, the load on the wafer, the rate of flow or the concentration of the abrasive. It is then followed by a micro-polishing step. Figure 9 shows the different machines used for our process and an example of $LiNbO_3$/Quartz substrate characterized using an ultrasound transmission technique to evaluate the bounding quality.

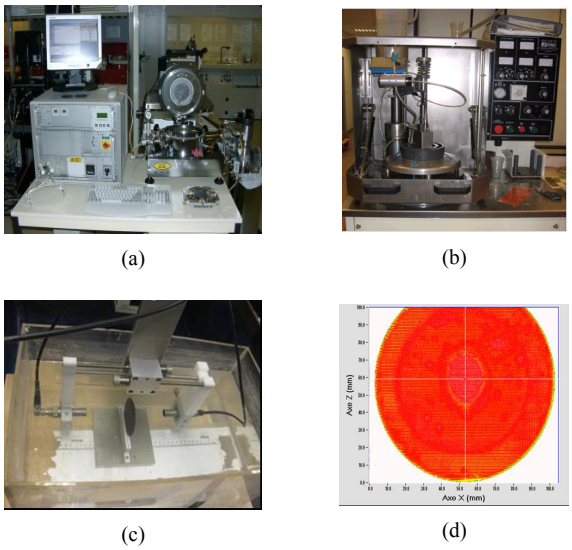

(a) (b) (c) (d)

Figure 9: Apparatus used for our process (a) wafer bounder (b) lapping/polishing (c) Ultrasonic bench for bounding characterization (d) example of a LiNbO3/Quartz bounding

Conforming to the above design and manufacturing process, several devices have been fabricated and tested to select the most appropriate one for frequency stabilization in the ISM band. Figure 10 shows one example of resonator admittance from which electromechanical coupling k_s^2 and Q factor are deduced, respectively at about 0.2% and 25 946, yielding a Q factor of 1.13×10^{13}, much better than Rayleigh wave based resonators on Quartz considering the same frequency. As shown in Fig.11 one can note that Q factor in excess of 14 000 also were measured at 1.27 GHz (QF near 2×10^{13}).

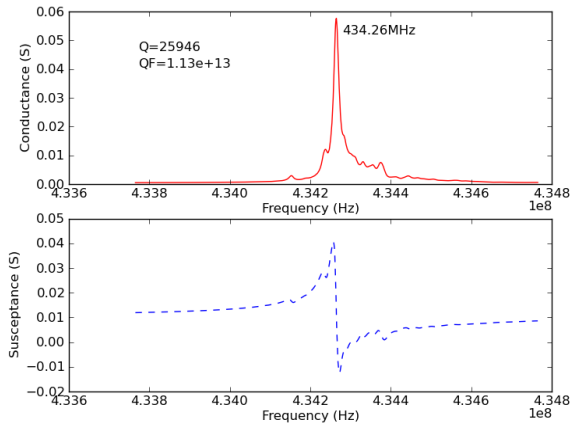

Figure 10: Experimental measurements (admittance) of a HBAR based on (YXl)/163° $LiNbO_3$ plate onto 350µm thick (YXlt)/34°/90° Quartz near the 434MHz-centered ISM band

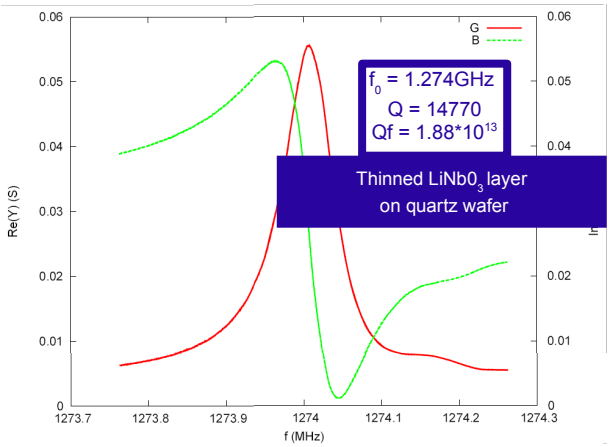

Figure 11: Experimental measurements (admittance) of a HBAR based on (YXl)/163° $LiNbO_3$ plate onto 350µm thick (YXlt)/34°/90° Quartz above 1 GHz

The TCFs have been again tested to demonstrate the predicted compensation effect, as shown in fig.12 as well as the possibility for controlling HBAR TCF along crystal cuts. Negative as well as positive TCF can be obtained along the assembled crystal cuts and the polarization of the excited wave in the substrat (fast or slow shear mode, yielding negative or 2nd order compensated TCF).

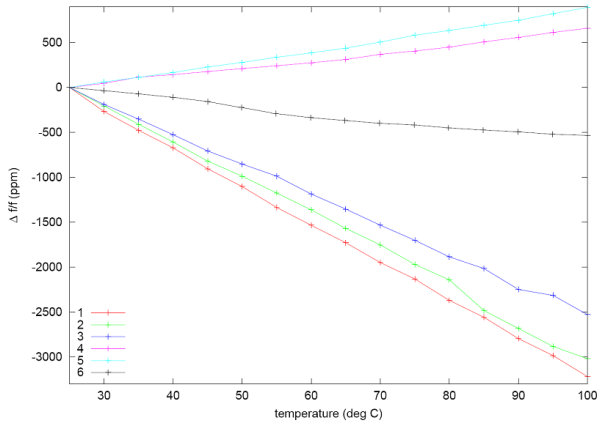

Figure 12: Frequency variation vs. temperature for various configurations of HBAR: compensation is achieved for (YX*l*)/163° $LiNbO_3$ on (YX*lt*)/34°/90° Quartz whereas a -30 ppm.K^{-1} TCF is measured for (YX*l*)/163° $LiNbO_3$ on (YX*l*)/34° Quartz

Niobate/Quartz double port HBAR above 1 GHz

We present here the transfer function obtain on the following stack: (YX*l*)/163° $LiNbO_3$ layer on a (YX*lt*)/36°/90° quartz plate. The electrodes defining the coupled transducers are two half-circles (diameter 300µm) separated by a gap of 20µm.

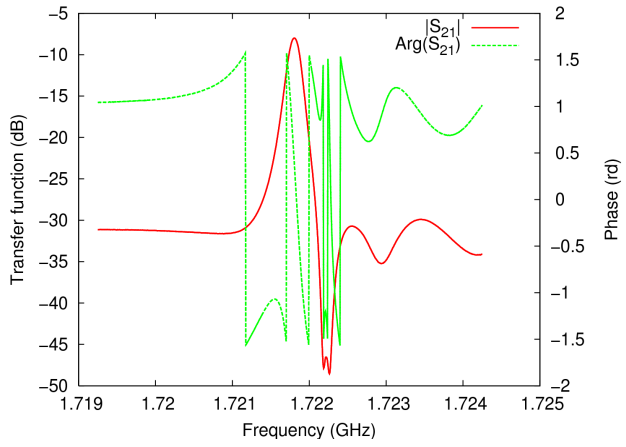

Figure 13: Transfer functions of laterally-coupled-mode HBAR near the third (top) and fifth (bottom) harmonics of the fundamental mode of the transducer, Q=10 128, IL=-8dB at 1.72GHz

In a previous work [8], it was observed that at lower frequency, two poles appear clearly in the peaks, which is advantageous for filter applications. However, the upper the frequency, the less clearly were appearing the two poles. Now, above 1GHz, one cannot distinguish the two modes anymore, but their influence can be still confirmed by the fact that the peak is broadened and the quality factor is smaller than at higher frequencies (Q<5000). At 1.7GHz (fig.13), the peak is thinner and it is clear that this structure is not suited anymore to filtering functions. However, the 8 dB insertion loss and the quality factor in excess of 10 000, which is much better than the values obtained using SAW quadripoles, shows that it is possible to stabilize an oscillator with this resonator.

Oscillator stabilization

Beside the high quality factor, the use of proper materials (niobate on quartz) enables temperature compensation, yealding favorable conditions for using this device to stabilize an oscillator loop. Moreover, the four-port structure is easily looped using a wide band amplifier.

The device were cut and packaged, mounted in an oscillator loop, and measurements of phase noise were performed. Fig 14 shows the phase noise of two oscillators at frequencies of 935MHz and 1.636GHz stabilized using our HBARs, compared with the phase noise of an oscillator stabilized by a classical BAW resonator at 100MHz, "octar 507X100" from AR-Electronics. The oscillator at 1.6GHz clearly shows better performances than the one at 935MHz, with a noise lower than -140dB at 100kHz from the carrier. In order to compare the 100MHz oscillator with the 1.6GHz, the low frequency source has to be multiplied by 16, i.e. +12dB must be add to the noise level. It gives a level of -140dB at 50kHz which is not far from our solution but requires the above-metioned multiplication chain.

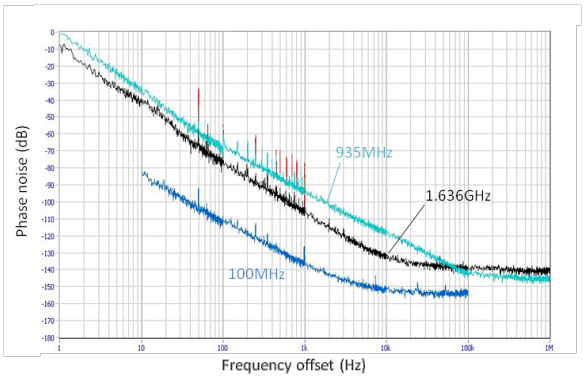

Figure 14: Phase noise curves for oscillators at 935MHz, 1.636MHz compared with the one of an oscillator based on a classical BAW resonator at 100MHz.

Stress sensor

One of the most regarded application of stress sensor is hydrostatic pressure measurements. In that matter, we have built a characterization bench simulating similar stress/strain effect than what occurs when bending a membrane by hydrostatic pressure. This bench allows for applying different mass at the back of the HBAR sensor near the micro-cavity location. Figure 15 shows this bench first developed to characterize SAW sensitivity to stress effects. The device is wire-bonded to a SMA connector to enable electrical measurements using a Rohde&Schwarz ZVR network analyzer. Once connected, the sensor is loaded by metallic disks of calibrated mass and the reflection coefficient S_{11} is recorded to characterize the device stress sensitivity. Figure 15 illustrates this experiment process and electrical response are reported in fig.6.

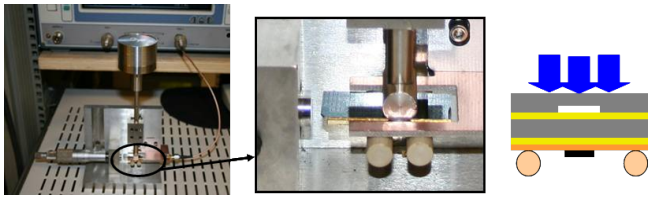

Figure 15: Photos and principle scheme of the mechanical bench for stress sensitivity characterization

Electrical responses as a function of applied mass show a shift of the resonance frequency of the HBAR. Figure 11 shows the electrical results and the shift of frequency vs mass loading on the device. The sensitivity of the device is found about 100 (±20) ppm per kg, This first result shows that the resonator actually can be designed to detect stress. However, many work still has to be achieved to definitely correlate the measurements with analysis and to characterize the effective stress sensitivity of the device. Nevertheless, this first experimental work has allowed to point out the main difficulties in the development of such a sensor (i.e. wafer alignment).

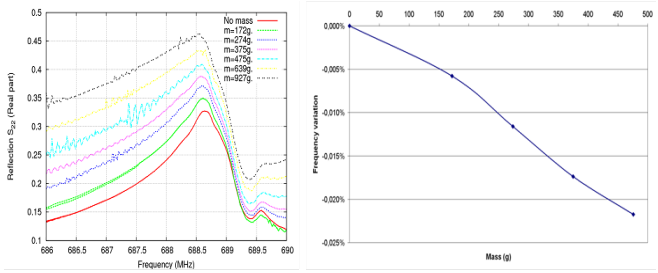

Figure 16: Electrical results: S_{11} magnitude variations vs. applied mass (left) and frequency variation vs applied mass.

Conclusion

In this paper, we have presented the interest of HBARs for various RF applications: filters, sources and sensors. The interest of HBAR devices mainly are related to their effective characteristics as well as their very small dimensions, yielding numerous advantages compared to usual RF devices (SAW in particular). Although their multi-mode signature generally is considered as a definitive drawback, we have proved that effective systems could be developed using such principles and resonators. We have shown the possibility to accurately control the temperature sensitivity of single-crystal HBAR structures. Such devices exhibit larger quality factor of their resonance together with larger coupling coefficients and an improved compactness than SAW resonators. Theoretical tools are available to optimize both the resonator electrical response and its thermal sensitivity. They also can be designed for stress measurements. In that latter application, more efforts are required to predict their actual sensitivity to stress. Non-linear elastic models will be then developed. Finally, oscillators have been developed, proving their capability for low phase noise figures, comparable with those of oscillators stabilized using standard solutions (SAW, BAW).

Acknowledgments

All these developments have been supported by the Centre National d'Etudes Spatiales (CNES) under grants #04/CNES/1941/00-DCT094 and #R-S08/TC-0001-026, by the Direction Générale pour l'Armement (DGA) under grant #05.34.016, by the FEDER (DIONYSOS) for the development of bounding/polishing techniques and by the the FCE – DGCIS under grant #092906659/60/61.

References

[1] Lakin, K. M. and Wang, J. S.: UHF composite bulk wave resonators. IEEE Ultrasonics Symposium Proceedings, :834-837,1980

[2] K.M. LAKIN: Thin film resonator technology. IEEE Trans. on UFFC, 52:707-716,2005

[3] S.P. CALDWELL, M.M. DRISCOLL, D. STANSBERRY, D.S. BAILEY, H.L. SALVO: High overtone bulk acoustic resonator frequency stability improvements. IEEE Trans. on UFFC, :744-748,1993

[4] D. Gachon, E. Courjon, G. Martin, L. Gauthier-Manuel, J.-C. Jeannot, W. Daniau and S. Ballandras, "Fabrication of high frequency bulk acoustic wave resonator using thinned single-crystal Lithium Niobate layers", Ferroelectrics, 362:30-40, 2008

[5] Curran Daniel R & Al, US Patent #3401275A, 1968-09-10

[6] M. Pijolat, D. Mercier, A. Reinhardt, E. Defaÿ, C. Deguet, M. Aïd, J.S. Moulet, B. Ghyselen, S. Ballandras, Mode conversion in high overtone bulk acoustic wave resonators, Proc. of the IEEE Ultrasonics Symp., pp.201-204, 2008

[7] T. Baron, E. Lebrasseur, J.P. Romand, S. Alzuaga, S. Queste, G. Martin, D. Gachon, T. Laroche, S. Ballandras, J. Masson, "Temperature compensated radio-frequency harmonic bulk acoustic resonators pressure sensors", IEEE Ultrasonics Symposium (IUS) 2010, pp. 2040-2043.

[8] D. Gachon, T. Baron, G. Martin, E. Lebrasseur, E. Courjon, F. Bassignot, S. Ballandras, "Laterally coupled narrow-band high overtone bulk wave filters using thinned single crystal lithium niobate layers", Frequency Control and the European Frequency and Time Forum (FCS), 2011

[9] J.J. Campbell, W.R. Jones, "A method for estimating crystals cuts and propagation direction for excitation of piezoelectric surface waves", IEEE Trans. On Sonics and Ultrasonics, Vol. 15, pp. 209-217, 1968

[10] T. Baron et al, A Pressure Sensor Based on a HBAR Micromachined Structure, Frequency Control Symposium (FCS), 2010 IEEE International , vol., no., pp.361-364, 1-4 June 2010 doi: 10.1109/FREQ.2010.5556312

[11] B.A Auld, Acoustic Fields and Waves in Solids, Vol I & II, 2nd edition Krieger Publishing Company, February 1990; ISBN: 089874783X